

High Resolution Spectroscopy of $^{16}_{\Lambda}\text{N}$ by Electroproduction

F. Cusanno,¹ G.M. Urciuoli,¹ A. Acha,² P. Ambrozewicz,² K.A. Aniol,³ P. Baturin,⁴ P.Y. Bertin,⁵ H. Benaoum,⁶ K.I. Blomqvist,⁷ W.U. Boeglin,² H. Breuer,⁸ P. Brindza,⁹ P. Bydžovský,¹⁰ A. Camsonne,⁵ C.C. Chang,⁸ J.-P. Chen,⁹ Seonho Choi,¹¹ E.A. Chudakov,⁹ E. Cisbani,¹² S. Colilli,¹² L. Coman,² B.J. Craver,¹³ G. De Cataldo,¹⁴ C.W. de Jager,⁹ R. De Leo,¹⁴ A.P. Deur,¹³ C. Ferdi,⁵ R.J. Feuerbach,⁹ E. Folts,⁹ R. Fratonì,¹² S. Frullani,¹² F. Garibaldi,¹² O. Gayou,¹⁵ F. Giuliani,¹² J. Gomez,⁹ M. Gricia,¹² J.O. Hansen,⁹ D. Hayes,¹⁶ D.W. Higinbotham,⁹ T.K. Holmstrom,¹⁷ C.E. Hyde,^{16,5} H.F. Ibrahim,¹⁶ M. Iodice,¹⁸ X. Jiang,⁴ L.J. Kaufman,¹⁹ K. Kino,²⁰ B. Kross,⁹ L. Lagamba,¹⁴ J.J. LeRose,⁹ R.A. Lindgren,¹³ M. Lucentini,¹² D.J. Margaziotis,³ P. Markowitz,² S. Marrone,¹⁴ Z.E. Meziani,¹¹ K. McCormick,⁴ R.W. Michaels,⁹ D.J. Millener,²¹ T. Miyoshi,²² B. Moffit,¹⁷ P.A. Monaghan,¹⁵ M. Moteabbed,² C. Muñoz Camacho,²³ S. Nanda,⁹ E. Nappi,¹⁴ V.V. Nelyubin,¹³ B.E. Norum,¹³ Y. Okasyasu,²² K.D. Paschke,¹⁹ C.F. Perdrisat,¹⁷ E. Piasetzky,²⁴ V.A. Punjabi,²⁵ Y. Qiang,¹⁵ B. Raue,² P.E. Reimer,²⁶ J. Reinhold,² B. Reitz,⁹ R.E. Roche,²⁷ V.M. Rodriguez,²⁸ A. Saha,⁹ F. Santavenerè,¹² A.J. Sarty,²⁹ J. Segal,⁹ A. Shahinyan,³⁰ J. Singh,¹³ S. Širca,³¹ R. Snyder,¹³ P.H. Solvignon,¹¹ M. Sotona,¹⁰ R. Subedi,³² V.A. Sulkosky,¹⁷ T. Suzuki,²² H. Ueno,³³ P.E. Ulmer,¹⁶ P. Veneroni,¹² E. Voutier,³⁴ B.B. Wojtsekhowski,⁹ X. Zheng,²⁶ and C. Zorn⁹

(Jefferson Lab Hall A Collaboration)

¹*Istituto Nazionale di Fisica Nucleare, Sezione di Roma, Piazzale A. Moro 2, I-00185 Rome, Italy*

²*Florida International University, Miami, Florida 33199, USA*

³*California State University, Los Angeles, Los Angeles California 90032, USA*

⁴*Rutgers, The State University of New Jersey, Piscataway, New Jersey 08855, USA*

⁵*Université Blaise Pascal/IN2P3, F-63177 Aubière, France*

⁶*Syracuse University, Syracuse, New York 13244, USA*

⁷*Universität Mainz, Mainz, Germany*

⁸*University of Maryland, College Park, Maryland 20742, USA*

⁹*Thomas Jefferson National Accelerator Facility, Newport News, Virginia 23606, USA*

¹⁰*Nuclear Physics Institute, Řež near Prague, Czech Republic*

¹¹*Temple University, Philadelphia, Pennsylvania 19122, USA*

¹²*Istituto Nazionale di Fisica Nucleare, Sezione di Roma, gruppo collegato Sanità, and Istituto Superiore di Sanità, I-00161 Rome, Italy*

¹³*University of Virginia, Charlottesville, Virginia 22904, USA*

¹⁴*Istituto Nazionale di Fisica Nucleare, Sezione di Bari and University of Bari, I-70126 Bari, Italy*

¹⁵*Massachusetts Institute of Technology, Cambridge, Massachusetts 02139, USA*

¹⁶*Old Dominion University, Norfolk, Virginia 23508, USA*

¹⁷*College of William and Mary, Williamsburg, Virginia 23187, USA*

¹⁸*Istituto Nazionale di Fisica Nucleare, Sezione di Roma Tre, I-00146 Rome, Italy*

¹⁹*University of Massachusetts Amherst, Amherst, Massachusetts 01003, USA*

²⁰*Research Center for Nuclear Physics, Osaka University, Ibaraki, Osaka 567-0047, Japan*

²¹*Brookhaven National Laboratory, Upton, New York 11973, USA*

²²*Tohoku University, Sendai, 980-8578, Japan*

²³*CEA Saclay, DAPNIA/SPhN, F-91191 Gif-sur-Yvette, France*

²⁴*School of Physics and Astronomy, Sackler Faculty of Exact Science, Tel Aviv University, Tel Aviv 69978, Israel*

²⁵*Norfolk State University, Norfolk, Virginia 23504, USA*

²⁶*Argonne National Laboratory, Argonne, Illinois 60439, USA*

²⁷*Florida State University, Tallahassee, Florida 32306, USA*

²⁸*University of Houston, Houston, Texas 77204, USA*

²⁹*St. Mary's University, Halifax, Nova Scotia, Canada*

³⁰*Yerevan Physics Institute, Yerevan, Armenia*

³¹*Dept. of Physics, University of Ljubljana, Slovenia*

³²*Kent State University, Kent, Ohio 44242, USA*

³³*Yamagata University, Yamagata 990-8560, Japan*

³⁴*LPSC, Université Joseph Fourier, CNRS/IN2P3, INPG, F-38026 Grenoble, France*

(Dated: October 29, 2018)

An experimental study of the $^{16}\text{O}(e, e'K^+)^{16}_{\Lambda}\text{N}$ reaction has been performed at Jefferson Lab. A thin film of falling water was used as a target. This permitted a simultaneous measurement of the $p(e, e'K^+)\Lambda, \Sigma^0$ exclusive reactions and a precise calibration of the energy scale. A ground-state binding energy of 13.76 ± 0.16 MeV was obtained for $^{16}_{\Lambda}\text{N}$ with better precision than previous measurements on the mirror hypernucleus $^{16}_{\Lambda}\text{O}$. Precise energies have been determined for peaks arising from a Λ in s and p orbits coupled to the $p_{1/2}$ and $p_{3/2}$ hole states of the ^{15}N core nucleus.

Hypernuclear spectroscopy is a powerful tool for studying the ΛN interaction ($N=p, n$) given that very limited information can be obtained from Yp ($Y = \Lambda, \Sigma^-, \Sigma^+$) elastic scattering and charge-exchange data [1].

Information on the spin-dependent part of the ΛN interaction can be extracted from the energy splitting of hypernuclear spin doublets formed when a Λ in an s state couples to a nuclear core state with non-zero spin. Seven such doublet splittings have been measured in ${}^7_\Lambda\text{Li}$, ${}^9_\Lambda\text{Be}$, ${}^{11}_\Lambda\text{B}$, ${}^{15}_\Lambda\text{N}$, and ${}^{16}_\Lambda\text{O}$ using an array of germanium detectors called the Hyperball [2, 3, 4, 5] and interpreted in terms of shell-model calculations that include both Λ and Σ hypernuclear configurations [6]. For ${}^{16}_\Lambda\text{O}$, the ground-state is found to have $J^\pi = 0^-$ with excited states at 26 keV (1^-), 6562 keV (1^-), and 6782 keV (2^-) [4, 5] (the 2^- state is weakly populated and its existence less certain).

More details of the effective ΛN interaction can in principle be obtained when the Λ is in a p state. With the exception of a $p_{1/2\Lambda}/p_{3/2\Lambda}$ doublet in ${}^{13}_\Lambda\text{C}$ [7], such states in p -shell nuclei are above particle thresholds and cannot be studied via γ -ray spectroscopy. Thus, experimental studies up until now have been carried out by hadron-induced reactions with limited energy resolution.

In fact, ${}^{16}\text{O}$ targets have been extensively used in hypernuclear studies with the (K^-, π^-) , (π^+, K^+) , and $(K_{\text{stop}}^-, \pi^-)$ reactions with dominant non-spin-flip reaction mechanisms that excite natural-parity states [2]. In all cases, four peaks are seen with the excited states at ≈ 6.2 , ≈ 10.6 , and ≈ 17.1 MeV corresponding to Λ 's in s and p orbits coupled to the $p_{1/2}^{-1}$ ground state and the 6.176-MeV $p_{3/2}^{-1}$ states of ${}^{15}\text{O}$. In the simple particle-hole limit, the degenerate multiplets contain 2, 2, 4, and 6 states, respectively, and the cross sections would be in the ratio 2:1 for peaks based on the $p_{3/2}$ vs. $p_{1/2}$ hole states. The first two peaks correspond to 1^- states and the B_Λ value for the lowest 1^- state is not particularly well determined. In the CERN (K^-, π^-) experiment [8], the third and fourth peaks correspond to substitutional 0^+ states. At the larger momentum transfer of the stopped K^- work at KEK [9], the same peaks contain contributions from both 0^+ and 2^+ hypernuclear states. Finally, in the (π^+, K^+) reaction, first performed at BNL [10] and later at KEK [2] with better energy resolution, only the 2^+ states are expected to contribute.

The experimental knowledge can be enhanced using the $(e, e'K^+)$ electroproduction reaction characterized by a large momentum transfer to the hypernucleus ($q \gtrsim 250$ MeV/c) and strong spin-flip terms, even at zero K^+ production angles, resulting in the excitation of both natural- and unnatural-parity states. In the present case, 1^- , 2^- , 1^+ , 2^+ , and 3^+ particle-hole states can be excited with significant cross sections. In addition, the $K^+\Lambda$ associated production occurs on a proton making ${}^{16}_\Lambda\text{N}$, the

mirror to ${}^{16}_\Lambda\text{O}$. After taking into account that the $p_{3/2}$ -hole state is 148 keV higher in ${}^{15}\text{N}$ than ${}^{15}\text{O}$, comparison of the energy spectra (and especially of Λ binding energies) of these mirror hypernuclei can, in principle, shed light on charge-dependent effects in hyperon-nucleon interactions.

The E94-107 experiment in Hall A at Jefferson Lab [11] started a systematic study of high resolution hypernuclear spectroscopy in the $1p$ shell region of nuclei, such as ${}^9\text{Be}$, ${}^{12}\text{C}$, and ${}^{16}\text{O}$. Results on ${}^{12}\text{C}$ have been published [12] and the results on ${}^{16}\text{O}$ are presented in this paper.

Hall A at JLab is well suited to perform $(e, e'K^+)$ experiments. Scattered electrons are detected in the High Resolution Spectrometer (HRS) electron arm while coincident kaons are detected in the HRS hadron arm [13]. The disadvantage of smaller electromagnetic cross sections is partially compensated for by the high current and high duty cycle capabilities of the beam. Throughout the experiment, the same equipment has been used in very similar kinematical conditions on C, Be, and H_2O targets. The use of a pair of septum magnets permitted particle detection at very forward angles [14] and a Ring Imaging Cherenkov (RICH) detector [15, 16, 17] has been used in the hadron arm to provide an unambiguous identification of kaons when combined with the standard particle identification apparatus of Hall A, based on aerogel Cherenkov detectors [18, 19, 20]. Details and motivations for the specific choices can be found in Ref. [12]. In the case of the waterfall target, the kinematics were set to particle detection at 6° for both electrons and kaons, incident beam energy of 3.66 GeV, scattered electron momentum of 1.45 GeV/c, and kaon momentum of 1.96 GeV/c. The electron beam current was about 60 μA . The spread of the beam energy was $< 3 \times 10^{-5}$, continuously monitored with a synchrotron-light interferometer [21].

In the present experiment, a waterfall target [22] was used because pure oxygen is difficult to handle and the use of other oxygen compounds requires additional measurements to subtract the non-oxygen background. The presence of the hydrogen has many advantages. In particular, it permits a calibration of the missing-mass scale and thus an accurate measurement of the Λ binding energy in the hypernucleus. Moreover, an interesting measurement of the $(e, e'K^+)$ cross section in a previously unmeasured kinematical region was possible.

A complete calibration of the target thickness as a function of pump speed has been performed, the thickness was determined from the elastic cross section on hydrogen [22]. The target thickness used was 75 ± 3 (stat.) ± 12 (syst.) mg/cm^2 . To calibrate the energy scale, the Λ peak position from the reaction on hydrogen was first obtained using the nominal central values for the kinematic variables, and then constrained to be zero by ap-

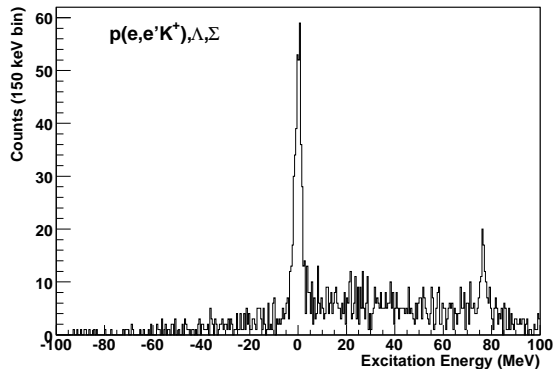


FIG. 1: Excitation energy spectrum of the $p(e, e'K^+)\Lambda, \Sigma^0$ on hydrogen, used for energy scale calibration. The fitted positions (not shown on the plot) for the peaks are -0.04 ± 0.08 MeV and 76.33 ± 0.24 MeV.

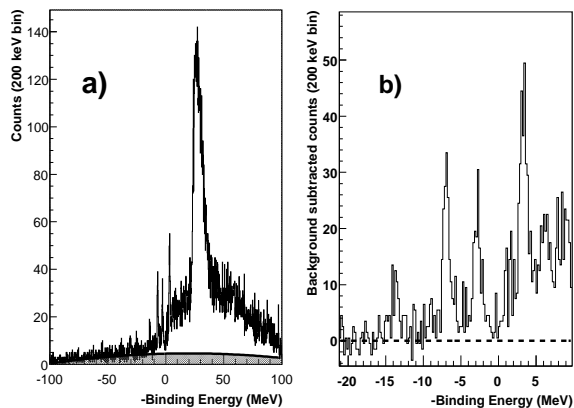


FIG. 2: The ${}^{16}_{\Lambda}\text{N}$ binding-energy spectrum obtained after kaon selection with aerogel detectors and RICH. The electron-kaon random coincidence contribution evaluated in a large timing window is superimposed on the spectrum in the left panel. The right panel shows the spectrum after this background has been subtracted.

plying a small shift to the energy of the beam (the quantity with the largest uncertainty). This shift is common to reactions on hydrogen and oxygen and therefore its uncertainty does not affect the determination of the binding energies of the ${}^{16}_{\Lambda}\text{N}$ levels. A resolution of 800 keV FWHM for the Λ peak on hydrogen is obtained. The linearity of the scale has been verified from the $\Sigma^0 - \Lambda$ mass difference of 76.9 MeV. For this purpose, a few hours of calibration data were taken with a slightly lower kaon momentum (at fixed angles) to have the Λ and Σ^0 peaks within the detector acceptance. Fig. 1 shows the two peaks associated with $p(e, e'K^+)\Lambda$ and $p(e, e'K^+)\Sigma^0$ production. The linearity is verified to $(76.9 - 76.4 \pm 0.3)/76.4 = 0.65 \pm 0.40\%$,

Figure 2 shows the binding-energy spectrum of ${}^{16}_{\Lambda}\text{N}$ for

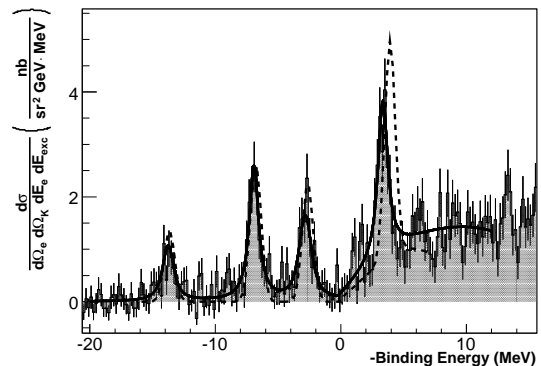


FIG. 3: The ${}^{16}_{\Lambda}\text{N}$ binding-energy spectrum. The best fit using Voigt functions (solid curve) and a theoretical prediction (dashed curve) are superimposed on the data. See text for details.

the full range of energy acceptance. The residual pion contamination is $< 5\%$, uniformly distributed over the energy spectrum (Fig. 2). The shaded region shows the $(e, e') \otimes (e, K^+)$ random-coincidence background. The large broad peak observed at around 30 MeV is the mis-reconstructed binding energy due to the contribution from the hydrogen when the oxygen mass is used for the target mass in constructing the missing mass. The excitation region of the ${}^{16}_{\Lambda}\text{N}$ production is shown on the right side of the figure. The background is rather flat. However, due to the acceptance of the detector, it decreases at the edges. It is separately evaluated by plotting the data obtained for random coincidences in a large energy window [12] and fit with a quadratic curve. No significant residual background is present after subtraction.

Figure 3 shows the six-fold differential cross section expressed in $\text{nb}/(\text{sr}^2 \cdot \text{GeV} \cdot \text{MeV})$. The fit to the data has been made using Voigt functions, as described elsewhere [12]. Four peaks are observed. The ground-state peak gives a Λ separation energy of $B_{\Lambda} = 13.76 \pm 0.16$ MeV for the 1^- member of the ground-state doublet in ${}^{16}_{\Lambda}\text{N}$. Three more peaks are observed at binding energies of 6.93, 2.84, and -3.34 MeV. The measured energies, widths, and cross sections, after a radiative unfolding procedure, are given in Table I. Only statistical errors are reported for the measured cross-sections. Systematic errors, dominated by uncertainty in the target thickness, are at the 20% level.

The theoretical cross sections were obtained in the framework of the distorted-wave impulse approximation (DWIA) [23] using the Saclay-Lyon (SLA) model [24] for the elementary $p(e, e'K^+)\Lambda$ reaction. The ground state of ${}^{16}\text{O}$ is assumed to be a simple closed shell and the shell-model wave functions for ${}^{16}_{\Lambda}\text{N}$ are computed in a particle-hole model space. For the $p_N^{-1}s_{\Lambda}$ states, a multi-range Gaussian (YNG) interaction (r^2 times a Gaussian for the tensor interaction) is adjusted to reproduce the

TABLE I: Excitation energies, widths, and cross sections obtained by fitting the $^{16}\text{O}(e, e'K^+)^{16}_\Lambda\text{N}$ spectrum (first three columns) compared with theoretical predictions (last four columns). The excitation energies of the remaining $p_N^{-1}p_\Lambda$ states, weakly populated by the $(e, e'K^+)$ reaction, are 11.17 (0^+), 11.27 (1^+), 17.21 (2^+), 17.27 (1^+), 17.67 (0^+), and 18.35 (1^+) MeV; note that spin-flip excitation for a $p_{3/2N} \rightarrow p_{3/2\Lambda}$ 2^+ transition is forbidden (17.21-MeV state).

E_x (MeV)	Experimental data		E_x (MeV)	Theoretical prediction		Cross section (nb/sr ² /GeV)
	Width (FWHM, MeV)	Cross section (nb/sr ² /GeV)		Wave function	J^π	
0.00	1.71 ± 0.70	1.45 ± 0.26	0.00	$p_{1/2}^{-1} \otimes s_{1/2\Lambda}$	0^-	0.002
			0.03	$p_{1/2}^{-1} \otimes s_{1/2\Lambda}$	1^-	1.45
6.83 ± 0.06	0.88 ± 0.31	3.16 ± 0.35	6.71	$p_{3/2}^{-1} \otimes s_{1/2\Lambda}$	1^-	0.80
			6.93	$p_{3/2}^{-1} \otimes s_{1/2\Lambda}$	2^-	2.11
10.92 ± 0.07	0.99 ± 0.29	2.11 ± 0.37	11.00	$p_{1/2}^{-1} \otimes p_{3/2\Lambda}$	2^+	1.82
			11.07	$p_{1/2}^{-1} \otimes p_{1/2\Lambda}$	1^+	0.62
17.10 ± 0.07	1.00 ± 0.23	3.44 ± 0.52	17.56	$p_{3/2}^{-1} \otimes p_{1/2\Lambda}$	2^+	2.10
			17.57	$p_{3/2}^{-1} \otimes p_{3/2\Lambda}$	3^+	2.26

spectra of $^{16}_\Lambda\text{O}$ and $^{15}_\Lambda\text{N}$ [5, 6] when matrix elements are evaluated with Woods-Saxon wave functions (with the s_Λ orbit bound by 13 MeV). This corresponds to fixing the conventional parameters Δ , S_Λ , S_N , and T for the spin-spin, Λ -spin-orbit, nucleon-spin-orbit, and tensor components of the ΛN interaction at (in MeV)

$$\Delta = 0.330 \quad S_\Lambda = -0.015 \quad S_N = -0.350 \quad T = 0.024. \quad (1)$$

The effect of Λ - Σ coupling is also taken into account [6]. The same YNG interaction is used for the $p_N^{-1}p_\Lambda$ states (with the p_Λ orbits bound by 2.5 MeV). There are now 13 independent matrix elements compared with 5 for $p_N^{-1}s_\Lambda$. Most of the new matrix elements involve relative d -wave states and are small. However, the relative s -wave and p -wave central matrix elements no longer appear in a fixed combination. Here, the choice of the odd-state central interactions is influenced by data on $^{13}_\Lambda\text{C}$ [7, 25].

The resulting energy spectra, dominant components of the wave functions, and calculated cross sections are shown in Table I. With respect to the calculations in [12], an improved optical potential (with stronger kaon absorption) for the high K^+ energy in these experiments has been used. The four pronounced peaks in the energy spectrum are reproduced by the shell-model calculation. It is significant that the energy separation between the two lowest peaks agrees very well with that deduced from the theoretical centroids, and hence with the precise γ -ray data [4, 5]. The excitation energies of the positive-parity states depend on the spacing of the p_Λ and s_Λ single-particle energies which have to be extrapolated from $^{13}_\Lambda\text{C}$ [7] and could therefore be uncertain by several hundred keV. The largest discrepancy between theory and experiment is in the position of the fourth peak. A firm prediction of the simple particle-hole model is that the gap between the third and fourth peaks should

be slightly larger (6.5 MeV) than the underlying separation (6.324 MeV) of the p -hole states in ^{15}N , in contrast to the observed splitting of 6.18 MeV. It remains to be seen whether a full $1\hbar\omega$ calculation, which includes s_Λ states coupled to positive-parity $1p2h$ states of the ^{15}N core, leads to significant energy shifts and some fractionation of the $p_N^{-1}p_\Lambda$ strength.

Historically, the first clear indication that the spin-orbit splitting of the p_Λ orbits is very small came from the observation that the separation between the 0^+ states is very close to the underlying core-state separation [8]. Table I shows that the predicted major contributors to the third and fourth peaks involve both the $p_{1/2\Lambda}$ and $p_{3/2\Lambda}$ orbits and are indeed closely spaced for a Λ -spin-orbit strength corresponding to the very small value of S_Λ in Eq. (1). Increasing the spin-orbit strength would eventually cause an observable broadening of the fourth peak. However, modest changes to any of the interaction parameters would not lead to deviations from the observed four-peak structure.

The Λ separation energy $B_\Lambda = 13.76 \pm 0.16$ MeV obtained for the first peak is to be compared with 13.3 ± 0.4 [26], 13.4 ± 0.4 [9, 27], and 12.4 ± 0.4 [2] for $^{16}_\Lambda\text{O}$ from in-flight and stopped K^- experiments. The new B_Λ value is an important quantity because *i)* it depends on the average central ΛN and perhaps ΛNN interactions in addition to the spin-dependence of the ΛN interaction that primarily affects energy level spacings, *ii)* there are few emulsion events for the heavier p -shell hypernuclei and these events tend to have ambiguous interpretations [28], and *iii)* the reactions involving the production of a Λ from a neutron are more difficult to normalize. For example, the (π^+, K^+) data are normalized to 10.80 MeV for the B_Λ of $^{12}_\Lambda\text{C}$ [2], which differs considerably from the much better determined value of 11.37 ± 0.06 MeV [28]

for the mirror hypernucleus ${}^{12}_{\Lambda}\text{B}$, and leads to B_{Λ} values [2] for ${}^7_{\Lambda}\text{Li}$, ${}^9_{\Lambda}\text{Be}$, ${}^{10}_{\Lambda}\text{B}$, and ${}^{13}_{\Lambda}\text{C}$ that are consistently lower than the emulsion values [28]. Thus, the value of 12.4 ± 0.4 MeV for ${}^{16}_{\Lambda}\text{O}$ may be an underestimate.

In summary, a high-quality ${}^{16}_{\Lambda}\text{N}$ hypernuclear spectrum has been obtained for the first time with sub-MeV energy resolution, thus putting tighter restrictions on the spacings of the levels contributing to each peak. The measured cross sections are in good agreement with the values predicted using the SLA model and simple shell-model wave functions. Most importantly, a B_{Λ} value for ${}^{16}_{\Lambda}\text{N}$ calibrated against the elementary ($e, e'K^+$) reaction on hydrogen, has been obtained.

We acknowledge the Jefferson Lab Physics and Accelerator Division staff for the outstanding efforts that made this work possible. This work was supported by U.S. DOE contract DE-AC05-84ER40150, Mod. nr. 175, under which the Southeastern Universities Research Association (SURA) operates the Thomas Jefferson National Accelerator Facility, by the Italian Istituto Nazionale di Fisica Nucleare and by the Grant Agency of the Czech Republic under grant No. 202/08/0984, by the french CEA and CNRS/IN2P3, and by the U.S. DOE under contracts, DE-AC02-06CH11357, DE-FG02-99ER41110, and DE-AC02-98-CH10886, and by the U.S. National Science Foundation.

[1] Th. A. Rijken, V. G. J. Stoks, and Y. Yamamoto, Phys. Rev. C **59**, 21 (1999).
 [2] O. Hashimoto and H. Tamura, Prog. Part. Nucl. Phys. **57**, 564 (2006).
 [3] H. Tamura *et al.*, Nucl. Phys. A **804**, 73 (2008).
 [4] M. Ukai *et al.*, Phys. Rev. Lett. **93**, 232501 (2004).
 [5] M. Ukai *et al.*, Phys. Rev. C, **77**, 054315 (2008).
 [6] D. J. Millener, Nucl. Phys. A **804**, 84 (2008).

[7] S. Ajimura *et al.*, Phys. Rev. Lett. **86**, 4255 (2001); H. Kohri *et al.*, Phys. Rev. C **65**, 034607 (2002).
 [8] W. Brückner *et al.*, Phys. Lett. B **79**, 157 (1978).
 [9] H. Tamura, R.S. Hayano, H. Outa, and T. Yamazaki, Prog. Theor. Phys. Suppl. **117**, 1 (1994).
 [10] P. H. Pile *et al.*, Phys. Rev. Lett. **66**, 2585 (1991).
 [11] F. Garibaldi, S. Frullani, P. Markowitz and J. LeRose, spokespersons, JLab Experiment E94-107, High Resolution 1p shell Hypernuclear Spectroscopy (1994).
 [12] M. Iodice *et al.*, Phys. Rev. Lett. **99**, 052501 (2007).
 [13] J. Alcorn *et al.*, Nucl. Instrum. Methods Phys. Res., Sect A **522**, 294 (2004).
 [14] G.M. Urciuoli, *et al.*, Nucl. Phys. A **691**, 43c (2001).
 [15] M. Iodice *et al.*, Nucl. Instrum. Methods Phys. Res., Sect A **553**, 231 (2005).
 [16] F. Garibaldi *et al.*, Nucl. Instrum. Methods Phys. Res., Sect A **502**, 117 (2003).
 [17] F. Cusanno *et al.*, Nucl. Instrum. Methods Phys. Res., Sect A **502**, 251 (2003).
 [18] R. Perrino *et al.*, Nucl. Instrum. Methods Phys. Res., Sect A **457**, 571 (2001).
 [19] L. Lagamba *et al.*, Nucl. Instrum. Methods Phys. Res., Sect A **471**, 325 (2001).
 [20] S. Marrone *et al.*, Nuovo Cimento B **124**, 99 (2009).
 [21] P. Chevtsov *et al.*, in *Proceedings of 2003 Particle Accelerator Conference*, Portland OR, USA, May 12-16 2003.
 [22] F. Garibaldi *et al.*, Nucl. Instrum. Methods Phys. Res., Sect A **314**, 1 (1992).
 [23] M. Sotona and S. Frullani, Prog. Theor. Phys. Suppl. **117**, 151 (1994).
 [24] T. Mizutani, C. Fayard, G.-H. Lamot, and B. Saghai, Phys. Rev. C **58**, 75 (1998).
 [25] E. H. Auerbach *et al.*, Phys. Rev. Lett. **47**, 1110 (1981); Ann. Phys. (NY) **148**, 381 (1983).
 [26] D.H. Davis and D.N. Tovee, fit to data from Ref. [8], private communication.
 [27] H. Tamura, erratum to Ref. [9], private communication.
 [28] D.H. Davis, in *LAMPF Workshop on (π, K) Physics*, edited by B.F. Gibson, W.R. Gibbs, and M.B. Johnson, AIP Conf. Proc. **224**, 38 (1991); D. H. Davis, Contemp. Phys. **27**, 91 (1986).